

Electronic Supporting information

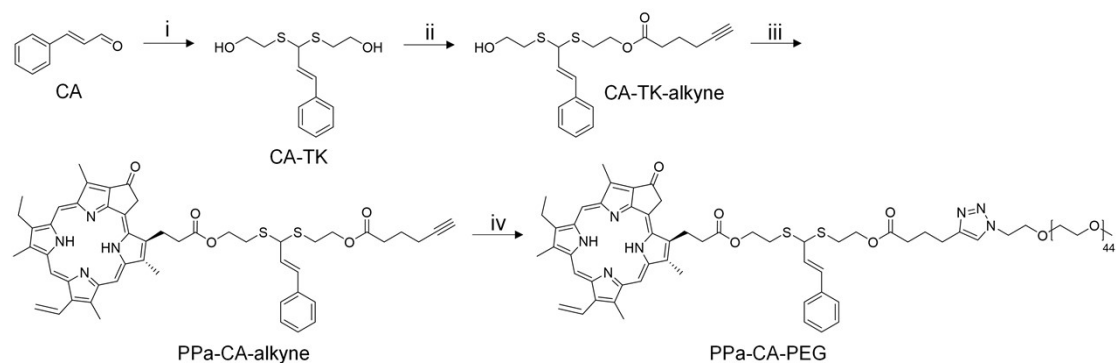
Self-Amplified Activatable Nanophotosensitizers for HIF-1 α
Inhibition-Enhanced Photodynamic Therapy

Zixin Guo, Nana Wang, Xiaowen He, Jinlong Shen, Xiangqi Yang, Chen Xie, Quli Fan, and Wen Zhou**

State Key Laboratory of Organic Electronics and Information Displays & Institute of
Advanced Materials (IAM), Nanjing University of Posts & Telecommunications, 9
Wenyuan Road, Nanjing 210023, China.

E-mail: iamqlfan@njupt.edu.cn; iamwzhou@njupt.edu.cn

1. Supporting figures



Scheme S1. Synthetic route of PPa-CA-PEG. Reagents and conditions: i) mercaptoethanol, trifluoroacetic acid, dichloromethane, room temperature, 12 h; ii) 5-hexynoic acid, N,N-dicyclohexylcarbodiimide, 4-dimethylaminopyridine, dichloromethane,

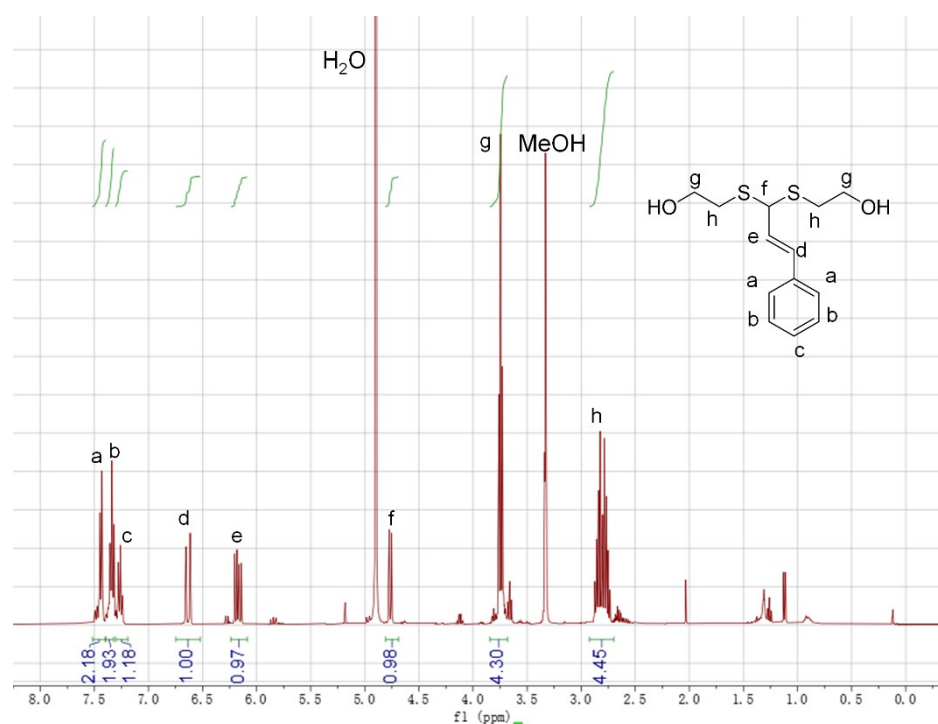


Figure S1. ¹H NMR spectrum of CA-TK. MeOH-d₄ was used as the solvent.

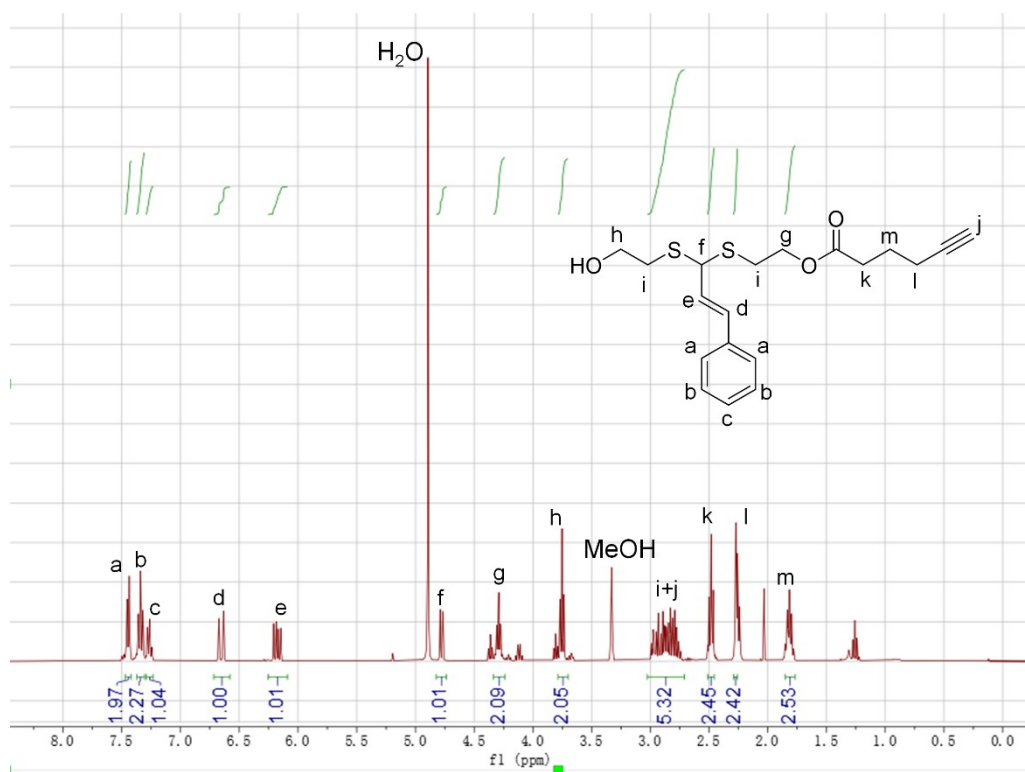


Figure S2. ¹H NMR spectrum of CA-TK-alkyne. MeOH-d₄ was used as the solvent.

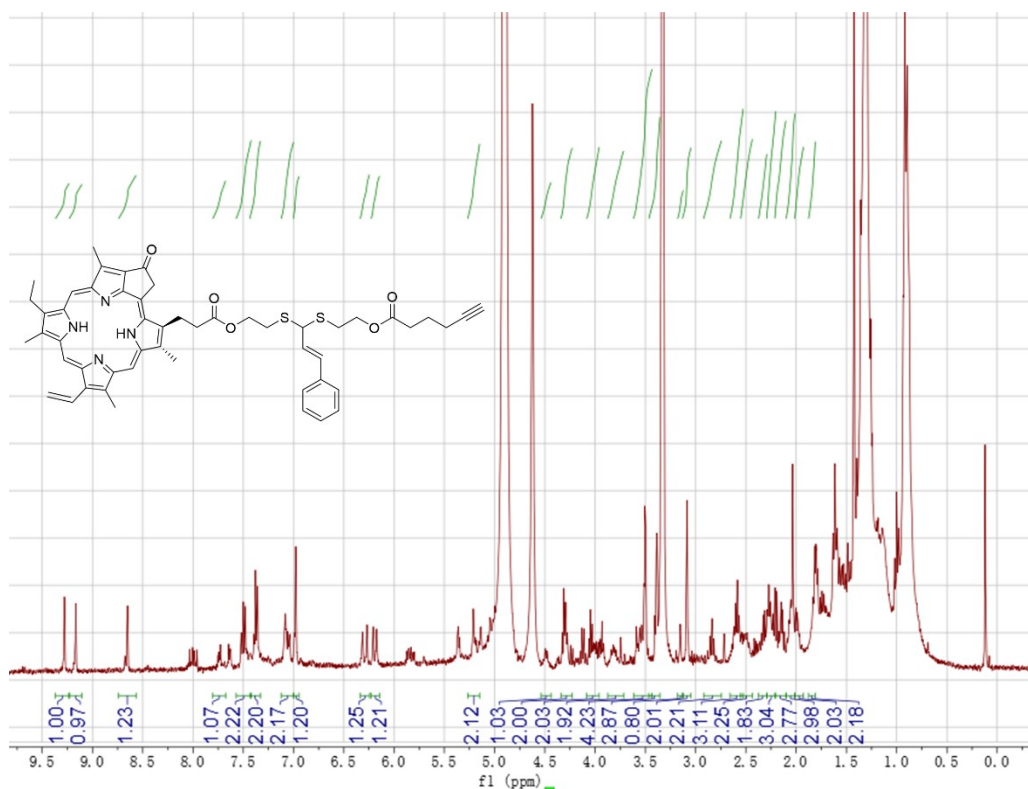


Figure S3. ¹H NMR spectrum of PPa-CA-alkyne. MeOH-d₄ was used as the solvent.

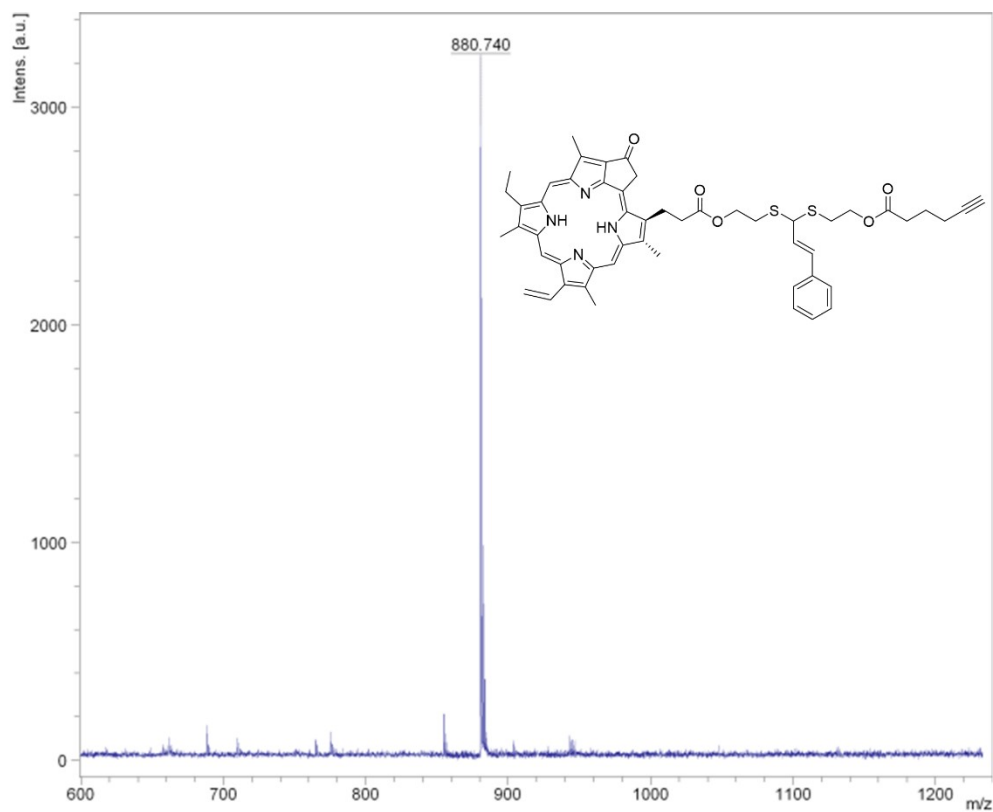


Figure S4. MALDI-TOF MS of PPa-CA-alkyne.

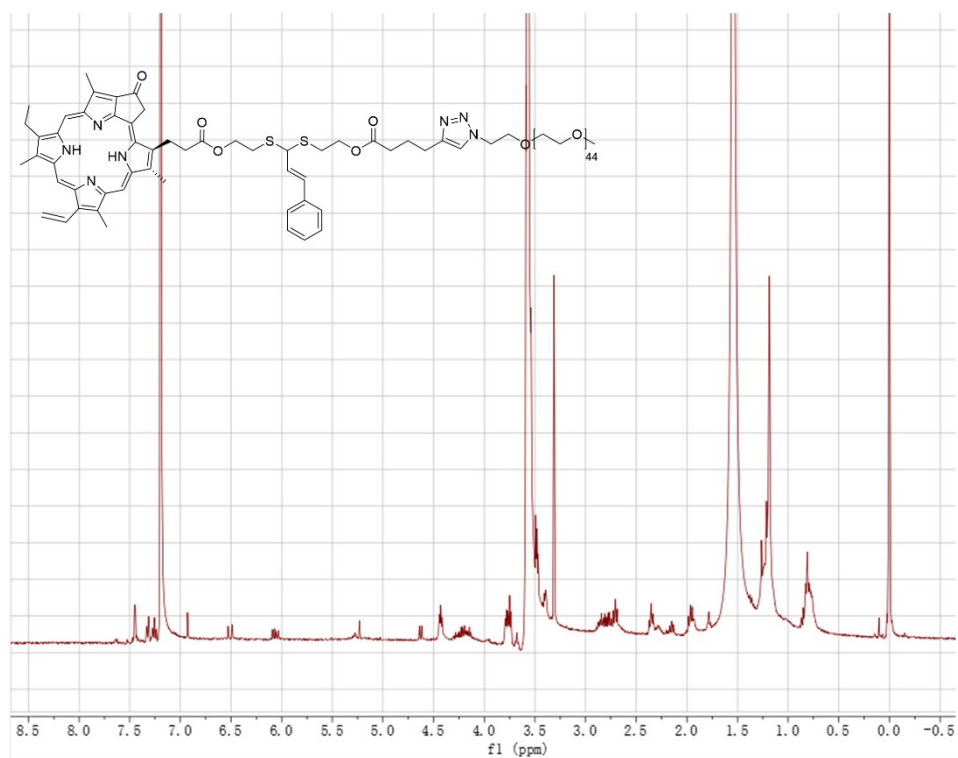


Figure S5. ^1H NMR spectrum of PPa-CA-PEG. CDCl_3 was used as the solvent.

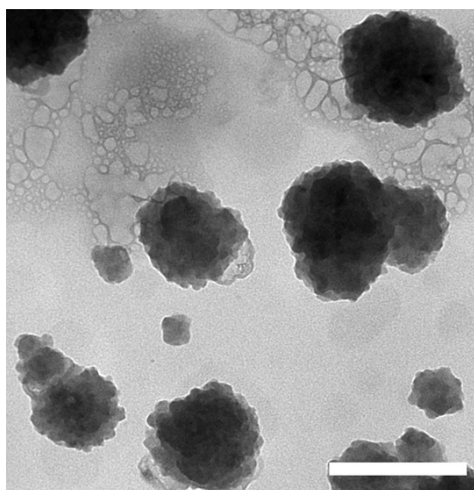


Figure S6. TEM image of CPPa NP after addition of H₂O₂. The scale bar represents 500 nm.

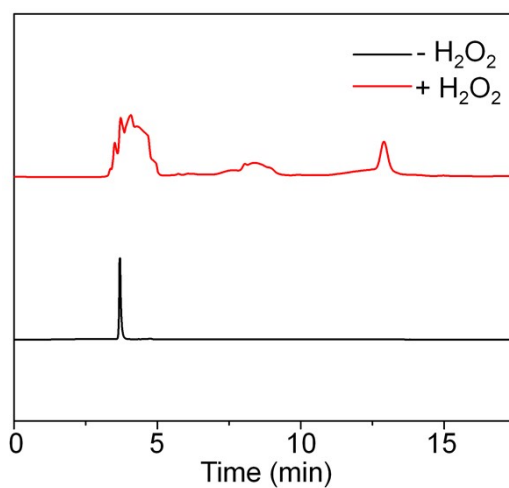


Figure S7. HPLC of PPa-CA-PEG before and after addition of H₂O₂.

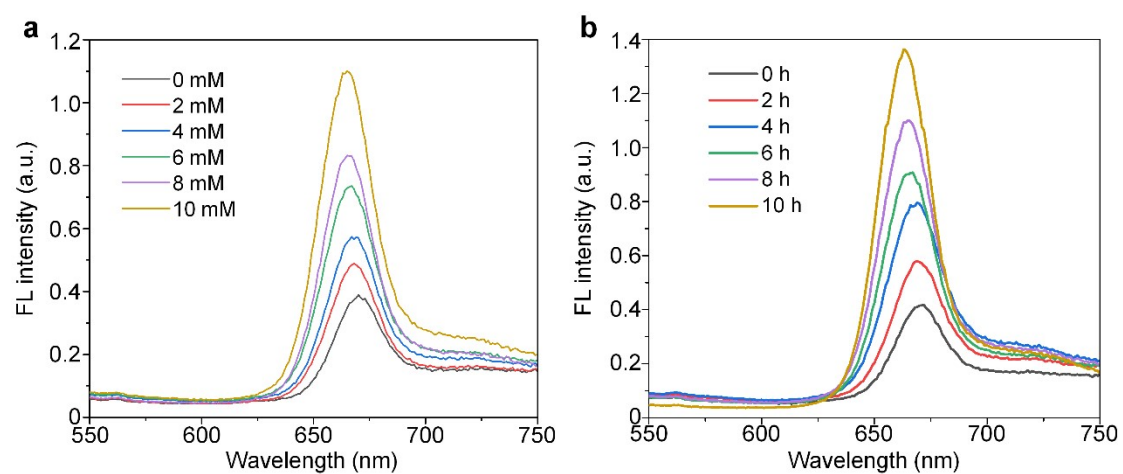


Figure S8. (a) Fluorescence spectra of CPPa NPs in the presence of HSA under

different concentrations of H_2O_2 . (b) Fluorescence spectra of CPPa NPs under the treatment of H_2O_2 (10 mM) and HSA at different incubation time.

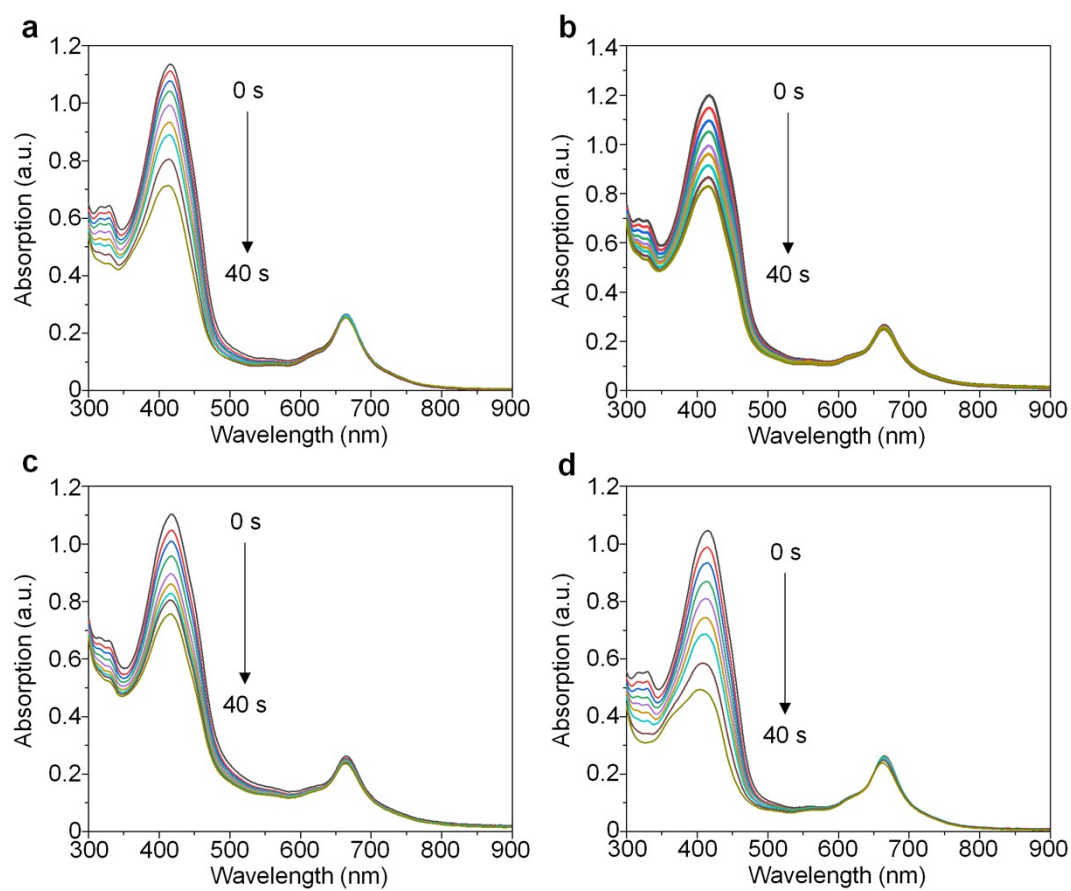


Figure S9. Absorption spectra changes of CPPa NPs incubated with DPBF with 635 nm laser irradiation time under the treatment of nothing (a), H_2O_2 (b), HSA (c) and H_2O_2 +HSA (d).

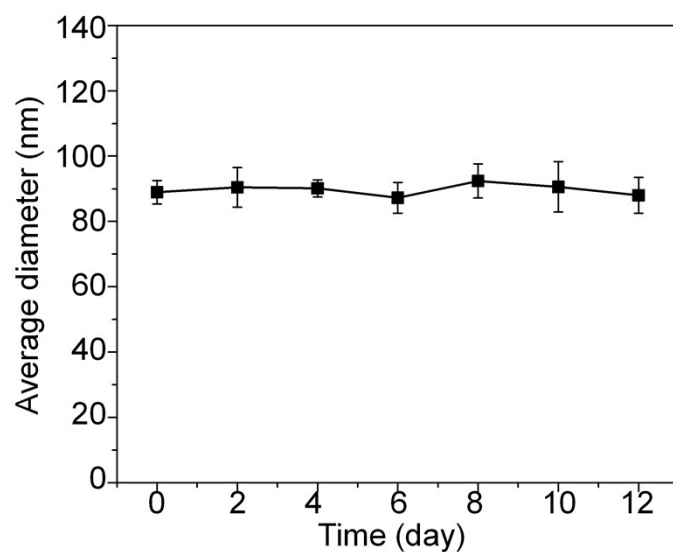


Figure S10. Average diameters of CPPa NPs in PBS solution under different storage times at 4 °C.

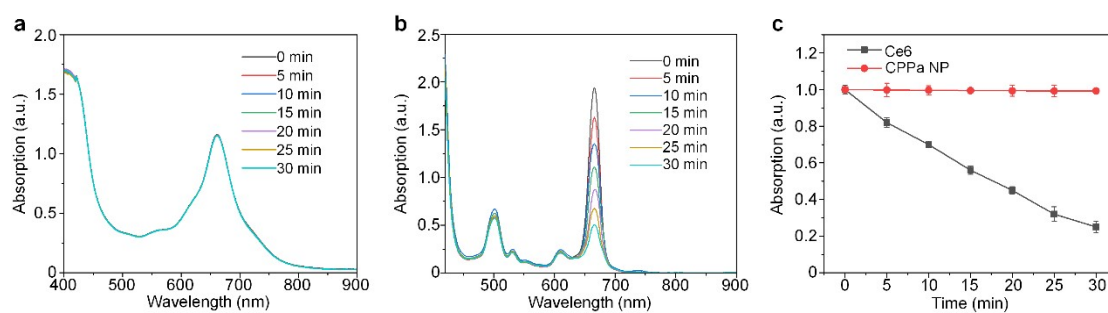


Figure S11. Absorption spectra of CPPa NP (a) and Ce6 (b) under different time of 635 nm laser irradiation. (c) Normalized maximum absorption changes of CPPa NP and Ce6 with laser irradiation time.

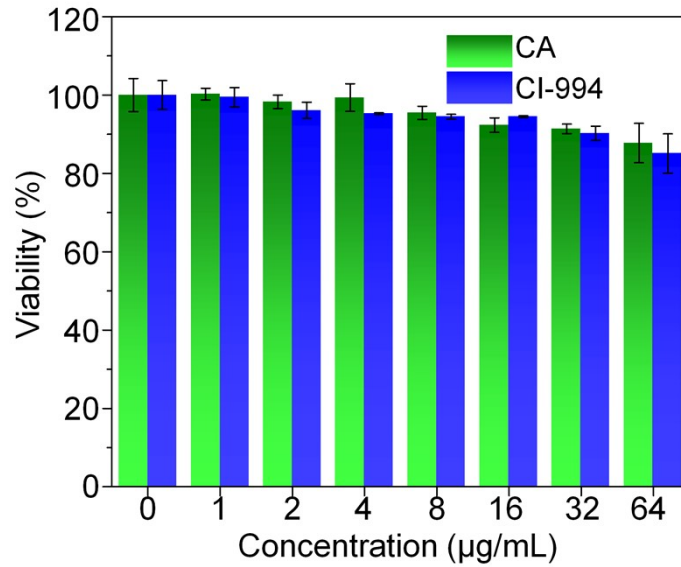


Figure S12. Viability of 4T1 cells under the treatment of different concentrations of CA or CI-994.

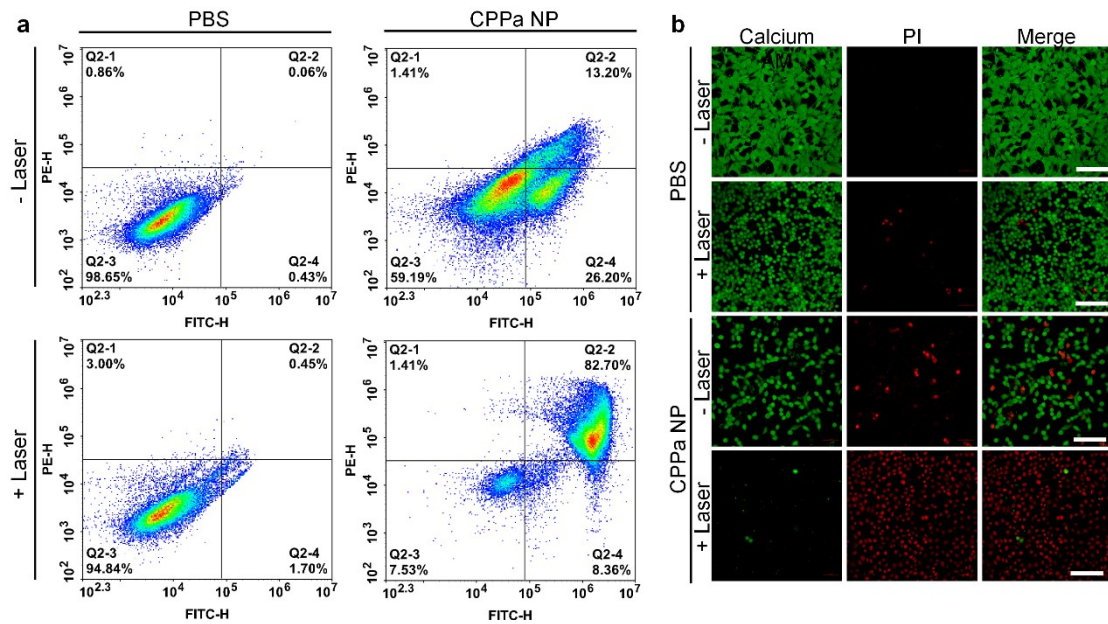


Figure S13. (a) Flow cytometry analysis for viability of 4T1 cells under different treatments. (b) Confocal fluorescence images of 4T1 cells under different treatments stained with Calcium-AM and PI. The scale bars represent 100 µm.

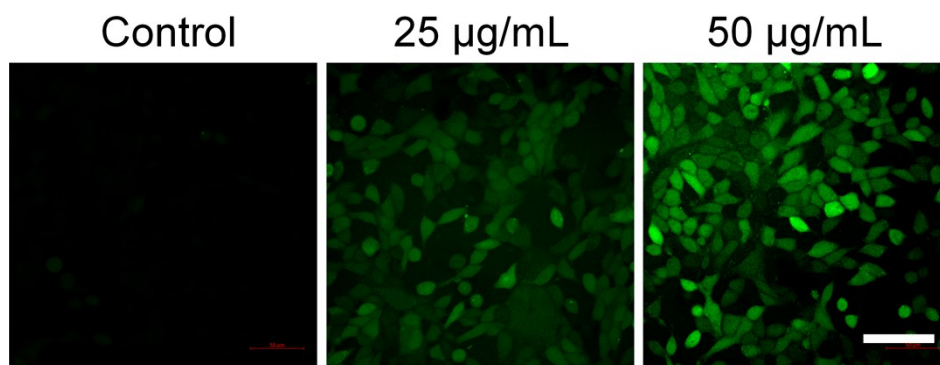


Figure S14. Confocal fluorescence images of DCFH-DA-treated 4T1 cells under the incubation of different concentrations of PPa NP for 12 h. The scale bars represent 100 μm .

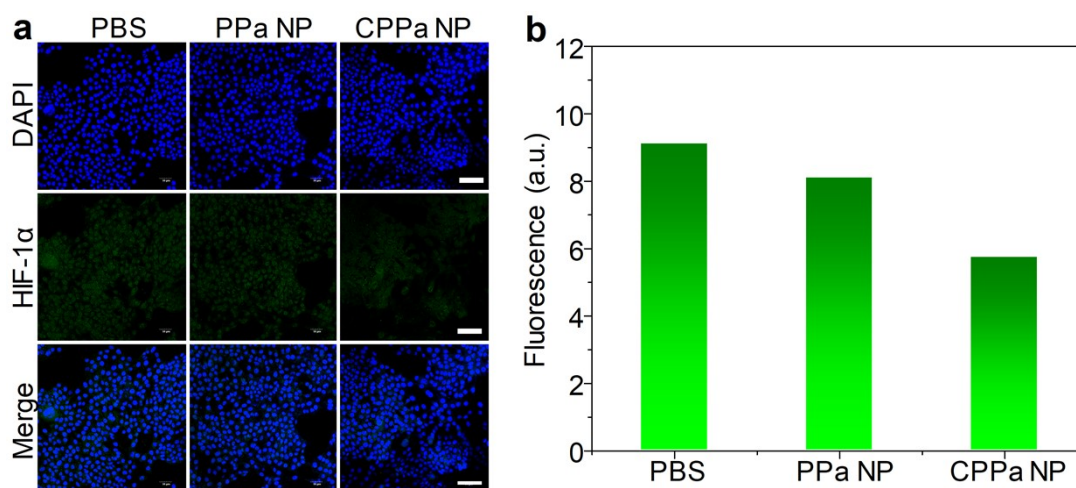


Figure S15. (a) Immunofluorescence staining of HIF-1 α within 4T1 cells with different treatments under normoxia. The green fluorescence indicates HIF-1 α , and the nuclei were stained with DAPI. The scale bars represent 100 μm . (b) Quantification result of green fluorescence intensity from figure a.

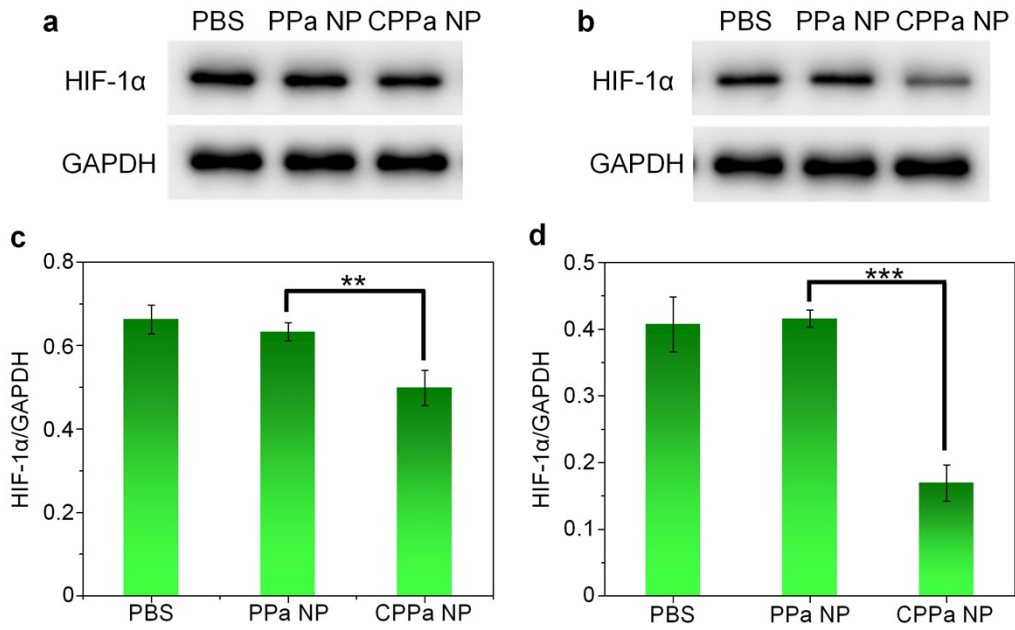


Figure S16. Western blotting of HIF-1 α protein within 4T1 cells after different treatment under normoxia (a) and hypoxia (b). Quantification results of HIF-1 α level under normoxia (c) and hypoxia (d) from (a) and (b), respectively. The error bars represent standard deviations of three separate measurements. **p < 0.01, ***p < 0.001.

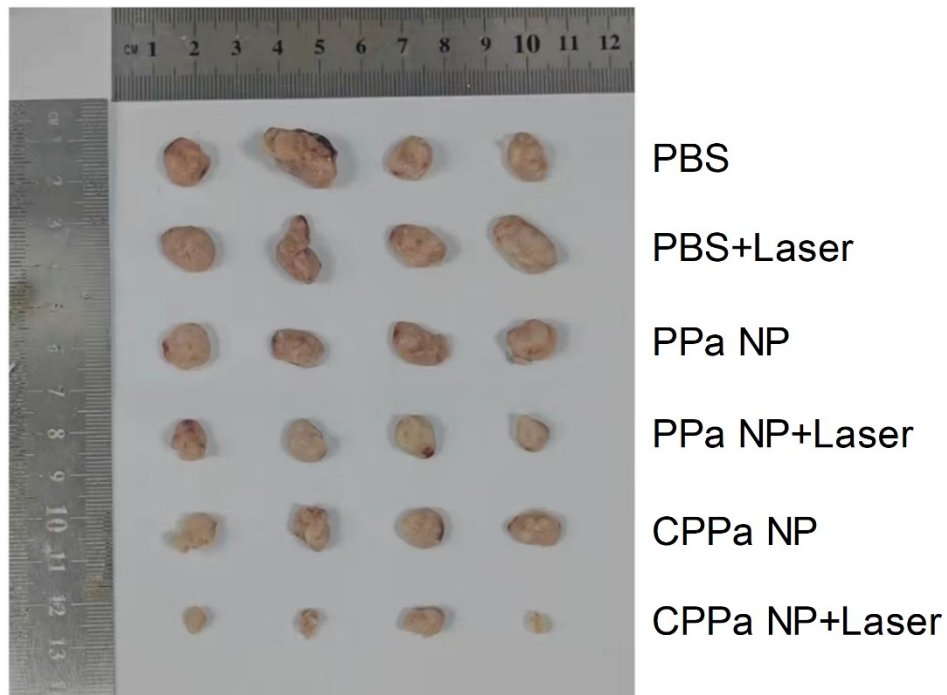


Figure S17. Image of tumor collected from different groups at t = 14 day post-

treatment.

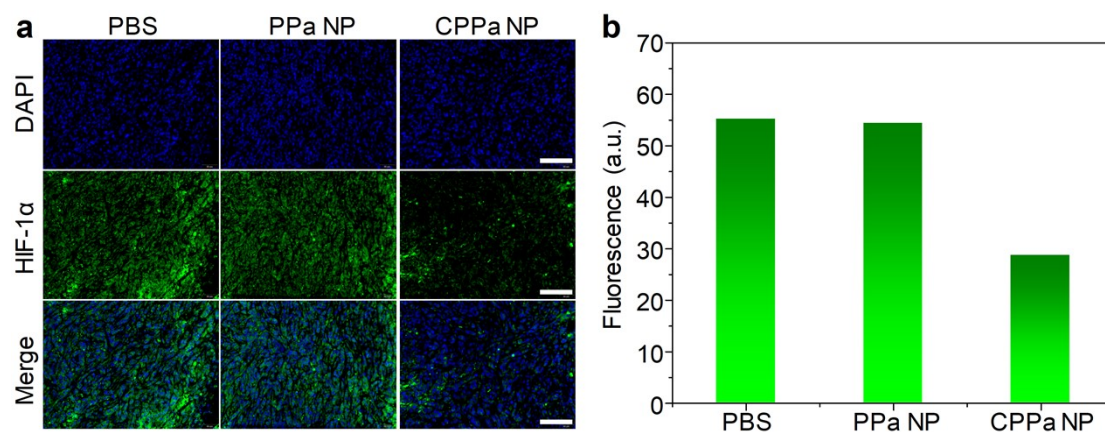


Figure S18. (a) Immunofluorescence staining of HIF-1 α within tumor tissue collected from 4T1 tumor bearing mice under different treatments. The scale bars represent 100 μ m. The cell nuclei were stained with DAPI. (b) Quantification result of green fluorescence intensity in figure (a).

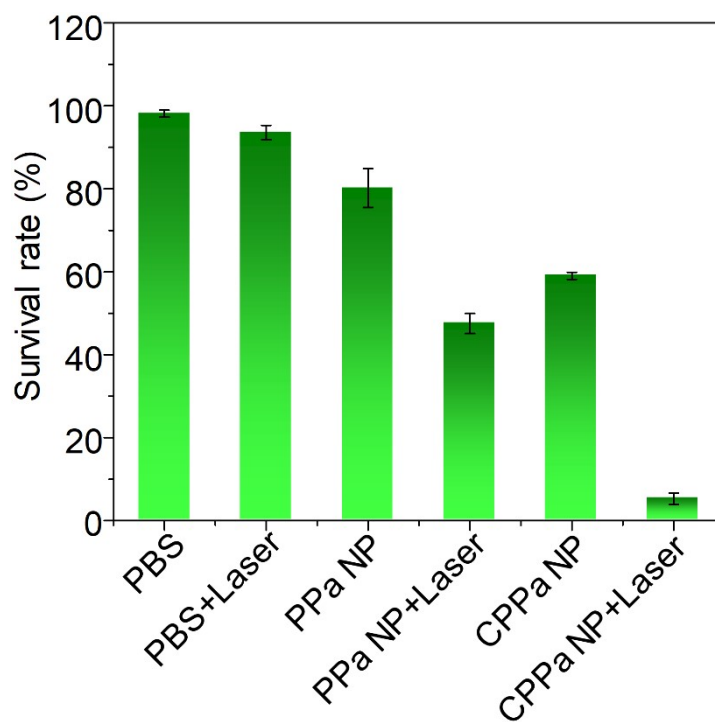


Figure S19. Survival rates of tumor cells from mice under different treatments.